ASCE

Understanding the Operating Speed Profile Patterns Using Unsupervised Machine Learning Approach: Short-Term Naturalistic Driving Study

Vinayak Malaghan[1]; Jahnavi Yarlagadda[2]; and Digvijay S. Pawar[3]

Abstract: Several studies have measured the minimum operating speed on horizontal curves to model the operating speed to assess the geometric design consistency. Most of these studies approximated equal lengths of deceleration and acceleration in the operating speed profiles for the curves and assumed the minimum operating speed position at the midpoint of the curve. In contrast, a few recent studies showed different percentages of deceleration lengths on the curve and measured the minimum operating speed at the deceleration end on the curve to model the operating speed. A defined pattern of the operating speed profile on the horizontal curve was not reported in the previous studies and therefore presents opportunities to determine the patterns of the operating speed profiles on curves. In this study, the operating speed profiles of different drivers for the given features of the horizontal curve were studied, and the clustering technique was used to categorize the different patterns in the operating speed profiles on horizontal curves. The optimal number of clusters was determined using four methods: silhouette, elbow, gap statistic, and NbClust function. The different patterns observed from the clustering results are as follows: (1) complete deceleration on the curve, (2) complete acceleration on the curve, (3) deceleration length slightly greater or lower than acceleration length, and (4) longer deceleration/acceleration lengths followed by shorter acceleration/deceleration lengths, respectively. The study results imply that all operating speed profiles are not symmetric around the midpoint of the curve (MC), and the group of drivers exhibited defined patterns of the operating speed profiles on the curves. This study helps in understanding the different patterns of operating speed profiles exhibited by the drivers and the measurement of the minimum operating speed at the deceleration end to model the operating speed to assess the geometric design consistency. **DOI: 10.1061/JTEPBS.TEENG-7440.** © *2022 American Society of Civil Engineers.*

Author keywords: Design consistency; Clustering; Minimum operating speed; Midpoint of the curve.

Introduction

The primary components of the highway mode of transport that contribute to road crashes are the driver, the road infrastructure, and the vehicle. Specifically, the road infrastructure component contributes to around 2.14 million road crashes in India (MORTH 2019). Previous studies showed that road crashes tend to concentrate on road geometric elements such as curves and tangent-to-curve transitions (Zegeer et al. 1992; Camacho-Torregrosa et al. 2013; Llopis-Castelló et al. 2018a, b). In India, fatal and nonfatal crashes on curved roads were reported to be approximately 20,000 and 60,000, respectively (MORTH 2019), underlining the importance of horizontal alignment design in preventing road crashes. One of the primary reasons for these road crashes is the lack of consistency in the geometric design standards that match the characteristics of the drivers and vehicles.

Therefore, the interaction between road users and road infrastructure has been widely studied in recent years. In this context, geometric design consistency is defined as how well the highway geometric design features match the characteristics of the drivers and vehicles that use the road (Garber and Hoel 2015; Malaghan et al. 2021a). A consistent roadway designed to meet the characteristics of drivers results in homogenous and harmonious driving operations and, thereby, safe maneuvers. In contrast, an inconsistent roadway causes sudden variations in the operating speed, causing critical maneuvers and increasing the likelihood of crash occurrence (Malaghan et al. 2020a).

Operating speed is one of the widely used measures in evaluating geometric design consistency (Fitzpatrick et al. 2000). The initial step in the operating speed measure is to develop the operating speed models for tangents, curves, and tangent-to-curve transitions. In developing the models, the maximum operating speed (speed at the beginning of deceleration) and minimum operating speed (speed at the end of deceleration) are measured on the tangent and curve, respectively (Pérez Zuriaga et al. 2010; Malaghan et al. 2021a).

Several studies assumed a constant operating speed on the horizontal curve and the entire acceleration/deceleration to be completed on the departure/approach tangent (Ottesen and Krammes 2000; Fitzpatrick and Collins 2000). Based on the aforementioned assumption, the operating speeds were measured at the midpoint of the curve (MC) and tangent to model operating speed for the geometric elements (tangent, curve, and tangent-to-curve transition) (Krammes et al. 1995; Passetti and Fambro 1999). However,

[1]Postdoctoral Researcher, Transportation Systems Engineering, Dept. of Civil Engineering, Indian Institute of Technology Hyderabad, Kandi, Medak, Telangana 502285, India; Assistant Professor, Transportation Engineering, Dept. of Civil Engineering, Pandit Deendayal Energy Univ., Gandhinagar, Gujarat, 382355, India (corresponding author). ORCID: https://orcid.org/0000-0002-7466-9140. Email: vinayakmalagahan@gmail.com

[2]Research Scholar, Transportation Systems Engineering, Dept. of Civil Engineering, Indian Institute of Technology Hyderabad, Kandi, Medak, Telangana 502285, India. Email: jahnavi.yarlagadda@gmail.com; ce17resch11013@iith.ac.in

[3]Assistant Professor, Transportation Systems Engineering, Dept. of Civil Engineering, Indian Institute of Technology Hyderabad, Kandi, Medak, Telangana 502285, India. Email: dspawar@ce.iith.ac.in

Note. This manuscript was submitted on March 23, 2022; approved on October 17, 2022; published online on December 15, 2022. Discussion period open until May 15, 2023; separate discussions must be submitted for individual papers. This paper is part of the ***Journal of Transportation Engineering, Part A: Systems***, © ASCE, ISSN 2473-2907.

studies invalidated the assumption of operating speed being constant on the horizontal curve and concluded that the deceleration continued even inside the horizontal curve (Pérez Zuriaga et al. 2010; Malaghan et al. 2021a). In addition, most studies assumed the lengths of deceleration and acceleration on the horizontal curve to be approximately equal (Figueroa Medina and Tarko 2007; Jacob and Anjaneyulu 2013; Sil et al. 2020). In other words, the pattern of the operating speed profile was assumed to be approximately symmetric about the MC on the horizontal curve (Figueroa Medina and Tarko 2007).

However, several recent studies showed that the deceleration end (or position of minimum operating speed) in every operating speed profile might not coincide with the MC, i.e., every operating speed profile might not be symmetric about the MC (Dhahir and Hassan 2018; Malaghan et al. 2021a). The percentage length of deceleration and acceleration transitions were random and varied across several past and recent studies (Figueroa Medina and Tarko 2007; Pérez-Zuriaga et al. 2013; Bella 2014; Dhahir and Hassan 2018). Therefore, a defined pattern or patterns of the operating speed profile on the horizontal curve were not observed (Fitzpatrick et al. 2000; Ottesen and Krammes 2000).

With this motivation, this study investigated whether the drivers exhibit a defined pattern or patterns of operating speed profiles on the horizontal curve. Therefore, in this study, the vehicles were instrumented with a Global Positioning System (GPS) device to record the continuous operating speeds along the trajectory on the selected road sections. The operating speed profiles on different horizontal curves between point of curvature (PC) and point of tangency (PT) were extracted, and an unsupervised machine learning approach was used to cluster the operating speed profiles with similar patterns.

The positions of maximum (or beginning of deceleration) and minimum (or end of deceleration) operating speeds on the tangent and curve, respectively, depend on the patterns of the operating speed profiles. Understanding the patterns of the operating speed profiles allows measuring the maximum/minimum operating speed accurately to develop reliable operating speed models and thereby promote the geometric design consistency evaluation in road safety.

This paper is structured in different sections as follows. Background and problem statement of this study is presented in "Introduction" section. "Literature Review" section provides a brief review of the hierarchy in the literature on operating speed profiles based on the type of device used. The research gaps from the literature scoping further work are presented in "Research Gaps and Objective" section. "Research Methodology" section details the research methodology required to achieve the objective stated in the previous section. The analysis results showing the clustering of the operating speed profiles with similar patterns are shown in the section, "Analysis of Operating Speed on Horizontal Curves." "Grouping of Patterns in the Operating Speed Profiles on Horizontal Curves" section groups the operating speed profiles with similar patterns from all the clusters. A brief discussion of the results from this study and relevant past studies is presented in "Discussion" section. The research contribution is presented in "Research Contribution" section. The conclusions from the analysis results of this study are listed in "Summary and Conclusion" section. Finally, this study has a few limitations, which are pointed out in "Limitations and Future Research Scope" section as a scope for future research work.

Literature Review

Operating speed is the commonly used measure to evaluate the geometric design consistency of rural highways (Camacho-Torregrosa et al. 2013; Llopis-Castelló et al. 2018a; Dhahir and Hassan 2018; Malaghan et al. 2020a, b). The speed at which drivers are observed to operate their vehicles under favorable weather and prevailing traffic conditions is referred to as operating speed. It is calculated as the 85th percentile value of the observed operating speeds at a specified locations (AASTHO 2011). The devices used to measure the operating speed in analyzing the operating speed profiles can be broadly categorized into three types: spot speed devices, driver simulators, and GPS devices equipped in vehicles.

Lamm et al. (1988) measured spot speeds at 11 spots on the approach tangent from the PC. They investigated the deceleration and acceleration movements from tangent to curve and curve to tangent, respectively. They found that the influence of curve features on the tangent operating speed extended 213 to 229 m from the ends of the curve. Their study assumed the operating speed to be constant on the horizontal curve and completion of acceleration/deceleration on the departure/approach tangent. The assumption of a constant operating speed profile (without any speed variations) on the horizontal curve was supported without any statistical validation, albeit an operating speed difference of 6.4 to 8.1 km/h at the curve ends.

Based on the aforementioned assumption and the available length of tangent between the curves, Ottesen and Krammes (2000) categorized the patterns of operating speed profiles into three generalized cases. In Case 1, the drivers' acceleration (or deceleration) pattern is linear (or uniform) between the consecutive curves for shorter tangents. In Case 2, the drivers accelerate and decelerate uniformly between the curves, but the length of the tangent is not long enough to attain and sustain the desired speeds. In Case 3, the tangent length is long enough for drivers to accelerate and sustain the desired speed, followed by a uniform deceleration. The acceleration and deceleration rates were assumed to be equal to 0.85 m/s^2, as proposed by Lamm et al. (1988). In all three cases, the operating speed on the horizontal curve was assumed constant without any variation in the speed.

Similarly, Fitzpatrick and Collins (2000) generalized the operating speed profiles into six cases based on different acceleration and deceleration conditions on the tangents between the consecutive curves. They estimated the acceleration/deceleration rate and presented equations to draw the operating speed profiles. The generalized pattern of the operating speed profiles also assumed a constant operating speed on the horizontal curve and completion of deceleration or/and acceleration on the tangents.

A report by the Transportation Research Board (TRB Operational Effects of Geometrics Committee 2011) presented a review of existing operating speed profile models developed over decades across different regions of the globe. The review's findings showed that most of the past studies developed 85th-percentile operating speed models for horizontal curves. In contrast, fewer studies developed models that estimated operating speeds on the tangents. Limited studies considered the combination of horizontal and vertical alignments to estimate the operating speed. The majority of studies assumed the operating speed to be constant on the curves and entire acceleration/deceleration to occur on the approach/departure tangent. However, this assumption was not supported in further studies, and thus speed profile models were developed considering the variation of the operating speed on the curves.

Jacob and Anjaneyulu (2013) conducted a pilot study and concluded that the drivers decelerated inside the curve and attained the minimum operating speed around the midpoint of the curve within a 10-m trap length. They assumed approximately equal lengths of deceleration and acceleration on the horizontal curve. Figueroa Medina and Tarko (2007) generalized the operating speed profile to develop operating speed profile models. The generalization of the symmetric operating speed profiles from tangent to curve and curve to tangent was based on the following assumptions:

(1) drivers select their desired speed on the tangent based on the features of the geometric elements (tangent and curve), (2) drivers decelerate uniformly before the beginning of the curve based on the geometric features of the curve, (3) the deceleration continues inside the curve, and drivers attain their preferred constant operating speed about the MC for a certain distance depending on the curve features, and (4) drivers accelerate uniformly inside the curve and continue the uniform acceleration on the departure tangents until their preferred operating speed is attained. The results of their study indicated that 66% of the deceleration transition and 72% of the acceleration transition occurred on the approach and departure tangents, respectively.

As mentioned previously, studies inferred that the drivers attained minimum operating speed or ended deceleration at the MC. To investigate whether all the drivers attained the minimum operating at the MC, McFadden and Elefteriadou (2000) divided the horizontal curve into four quarters, and the spot speed was measured at five locations to determine the position of the minimum operating speed on the horizontal curve. The results of their study showed that the drivers attained the minimum operating speed at any of the five locations on the horizontal curves. This implies that every operating speed profile might not be symmetric about the MC on the horizontal curve.

Spot speed devices allow the measurement of a speed value at a specific point on a given length of the geometric elements. This limitation can be overcome by using driving simulators or vehicles equipped with a GPS device that allows recording continuous speed data along the vehicle's trajectory.

Several studies based on driving simulators analyzed the operating speed profiles on the curve and from tangent to the curve and curve to the tangent (Montella et al. 2014a; Bella 2014; Wang et al. 2020). Montella et al. (2014a) obtained 357 operating speed profiles for the tangent-to-curve transitions. The most recurring behaviors were the beginning of deceleration on the approach tangent and the end of deceleration on the spiral transition. Other commonly observed behaviors included (1) the beginning and ending of the deceleration on the approach tangent; and (2) the beginning and ending of the deceleration on the approach tangent and first quarter of the curve, respectively. The average percentage of deceleration length on the geometric elements was 59% on the approach tangent, 30% on the spiral transition, and 11% on the curve. In the case of acceleration, the average percent proportion on the geometric elements included (1) 2% before the circular curve, (2) 47% on the circular curve, (3) 18% on the spiral transition after the curve, and (4) 33% on the departure tangent.

Similarly, Bella (2014) obtained 856 operating speed profiles for the tangent-to-curve transitions. It was observed that the prevailing behaviors of drivers on the geometric elements were as follows: (1) the drivers kept their preferred operating speed on the approach tangent, (2) the drivers (83%) commenced deceleration as they approached the curve and completed the deceleration at some point (minimum operating speed position) inside the curve (74%), (3) the attainment of the minimum operating speed position depended on the features of the curve, and (4) the drivers started their acceleration inside the curve and continued acceleration (95%) until their preferred operating speed was attained on the tangent.

The studies based on driving simulators have limitations such as awareness of low risk, lack of dynamic visualization, and lack of motion perception. Therefore, vehicles are instrumented with GPS devices to overcome these limitations and obtain driver data in the real-world environment. However, the presence of a GPS device in a short-term naturalistic driving study might influence the drivers' behavior (Malaghan et al. 2021b; Dhahir and Hassan 2018).

Pérez Zuriaga et al. (2010) used a pocket-sized GPS device equipped on passenger cars to obtain continuous operating speed profiles along the trajectory of the vehicles. Using the speed profiles, the authors determined the operating speed at the beginning and end of deceleration and developed operating speed profile models. Their study results showed that 45% of the curve length was traversed in deceleration, and in 58% of the curve sites, the deceleration ended before the MC.

Another study by Pérez-Zuriaga et al. (2013) analyzed the speed profiles from tangent to the curve and developed operating speed profile models. The most common observed behavior was the beginning of deceleration on the tangents and ending inside the curve. The study results showed that 45% of the deceleration length occurred on the tangent and the remaining 55% on the curves. Similarly, a study by Montella et al. (2014b) analyzed 2,720 operating speed profiles for the tangent-to-curve transitions. They observed that 52% of the transitions in deceleration started on the approach tangent and ended inside the curve. In contrast, 90% of the transitions in acceleration started inside the curve. Among 90% of the transitions, 27% and 63% started before and after the MC, respectively.

Dhahir and Hassan (2018) studied driver behavior in terms of lateral and longitudinal acceleration and operating speed on the horizontal curves using naturalistic driving data. They stated that the trend in the operating speed profile varied based on the vehicle's relative position on the curve. Hence, the curve was divided into three equal zones, and the analysis of speed was carried on the zone that represented the general speed trend on the curve.

Previous literature did not analyze the distribution of minimum operating speed positions (or positions of the deceleration end) in the operating speed profiles on the horizontal curves. A recent study by Malaghan et al. (2021a) used instrumented vehicle data and analyzed the operating speed profiles on the horizontal curves. The distribution of the minimum operating speed positions was studied for the 22 horizontal curves. The results showed that the frequency of the positions of the minimum operating speed was high around the midcurve, which decreased toward the curve ends. The minimum operating speed position data on the majority of the horizontal curves followed a normal distribution. However, the patterns of the speed profiles on the horizontal curves were not presented. Hence, this study investigated whether a set of drivers exhibited a defined pattern or patterns of the operating speed profiles on the horizontal curves.

Research Gaps and Objective

To summarize, previous studies in the literature assumed constant operating speed on the horizontal curve. Fewer past and recent studies concluded that the deceleration might end around the midpoint of the curve, i.e., the acceleration and deceleration lengths of the operating speed profiles on the horizontal curve were assumed to be approximately equal. With advancements in technology, studies based on driving simulators and instrumented vehicles showed random variations in the percentage acceleration and deceleration lengths on the horizontal curves. Defined patterns of the operating speed profiles on the horizontal curve were not observed. Therefore, the primary objective of this study is to determine the patterns of the operating speed profiles on horizontal curves using an unsupervised machine learning approach.

Research Methodology

Test Routes and Geometric Data

Five two-lane rural highways comprising three state highways (SH), a national highway (NH), and a major district road (MDR) segments in the states of Karnataka and Telangana, India, were

Table 1. Summary of the horizontal alignment features of the selected road segments

Horizontal alignment features	Statistic	Type of road segments				
		NH 161	SH 17	SH 53	SH 135	MDR
Curve radius (m)	Range	200–900	150–300	60–500	90–800	60–200
	Mean	454.62	225	150	240.91	100
	SD	185.72	64.55	104.87	193.52	67.33
Curve length (m)	Range	90–785	135–200	45–310	60–225	40–105
	Mean	346.86	170.25	86.95	117.99	68.87
	SD	181.84	25.54	60.24	48.03	27.56
Deflection angle (degree)	Range	20–75	35–55	20–65	5–55	20–75
	Mean	45.55	44.73	35.62	34.09	46.53
	SD	17.45	6.51	12.19	13.52	21.45
Tangent length (m)	Range	465–3,655	100–1,065	20–840	220–1,420	120–1,040
	Mean	1,570	545	364.29	856.82	405.63
	SD	1,031.88	376.37	196.64	392.06	290.46
Length (m)		3,380	46,780	12,700	15,900	3,200
Number of curves		4	13	17	11	4

Note: MDR = major district road; SH = state highway; NH = national highway; and SD = standard deviation.

selected to perform the field experiment (Table 1). The total length of all the selected road segments was approximately 8,200 m. The chosen road segments were located in plain terrain. The existing horizontal alignment design features of the selected road sections were determined using highway geometric design tool AutoCAD Civil 3D 13.0 and Google Earth Pro software 7.3.3. The coordinates of position (latitude and longitude) along the centerline of the selected road section were obtained from the Google Earth Pro software. These coordinates were imported into AutoCAD Civil 3D to create a centerline of the selected road section. The centerline was referenced to create a Civil 3D alignment. The Civil 3D alignment overlapped the referenced centerline of the road. The Civil 3D alignment was edited for the radius to match the referenced centerline obtained from the coordinates of Google Earth Pro software.

The Civil 3D alignment provided the details of the positions of PC, MC, and PT. The primary horizontal alignment design data determined were curve length, curve radius, deflection angle, and tangent length. The summary of the descriptive statistics of the horizontal alignment design features of the chosen road segments is presented in Table 1. The secondary data of the selected road segments, such as lane width, number of lanes, type of shoulder, and width of paved/unpaved shoulder, were measured during field visits. The lane width of the selected road segments ranged from 3.0 to 3.5 m. The paved and earthen shoulder widths ranged from 1.0 to 1.5 m and 1.0 to 2.0 m, respectively. Past studies compared the free-flow speeds on the curves provided with and without spiral transitions and inferred no significant effect of spiral transitions on the 85th percentile operating speeds (Passetti and Fambro 1999; Russo et al. 2016). In this study, the horizontal alignment was determined to match the existing horizontal alignment of the chosen road sections. The horizontal curves in the selected road sections were designed as simple curves without spiral transitions. The following criteria to ensure the influence of road geometry on the operating speed were confirmed during the field visits:

- The curve sites in the selected road segments were away from the major/minor intersection.
- The curve sites in the chosen road segments were away from the merging/diverging approaches.
- The curve sites were away from the influence of narrow bridges, culverts, and the road overbridge/underbridge.
- The selected road segments represented low traffic volume.
- The selected road segments represented good pavement condition with proper road markings.

In-Vehicle Data

The in-vehicle data were collected using passenger cars instrumented with a 10-Hz GPS data logger (Fig. 1). The data were collected for different light motor vehicles, namely sports utility vehicles (SUVs), sedans, and hatchbacks grouped under a single-vehicle category called passenger cars. The primary components of the GPS device constituted an antenna, a camera, and a GPS box. The camera was fixed to the windshield below the rear-view mirror,

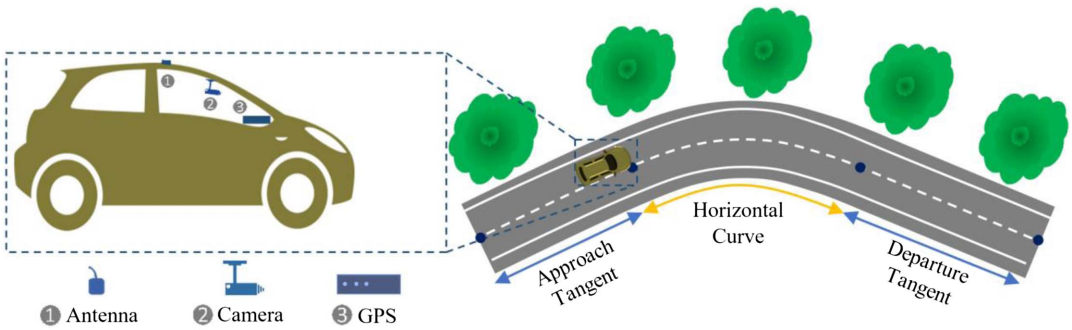

Fig. 1. Schematic representation of instrumented passenger car.

Table 2. Summary of the number of trips on the selected road segments

Road segments	No. of curves	No. of tangents	No. of independent tangents	No. of trips
MDR	4	6	5	54
SH 17	13	20	20	70
SH 53	17	24	17	87
SH 135	11	15	15	91
NH 161	4	5	4	48

the antenna was placed on the rooftop of the car, and the GPS box was placed near the dashboard, as shown in Fig. 1.

The in-vehicle data such as speed, position (latitude and longitude), longitudinal acceleration, lateral acceleration were recorded at every 0.1 s and stored in the memory card inserted in the GPS box. The camera recorded high-definition (HD) video (1,080 p video at 60 frames per second) of the surroundings in the direction of travel and weather conditions during the data collection period. The data were collected during the daytime under dry weather conditions. The number of the trips on the selected road segments ranged between 48 and 91, as detailed in Table 2.

Participant Profiles

To investigate the influence of road geometry on the operating speed of the drivers, a total of 49 male participants based on convenience sampling participated in the experiment. By occupation, the participants were professional taxicab drivers. The age of the participants ranged from 21 to 59 years, with a mean and standard deviation (SD) of 33.02 and 9.58 years. The participants' driving experience ranged from 1 to 38 years (counted from the driving license), with a mean of 12.60 years and a standard deviation of 9.77 years. The drivers were informed that the vehicle will be instrumented with a GPS device and the data obtained would be utilized for the university's research project and not for legal enforcement. Also, they were informed that the data obtained would remain anonymous. In this way, the drivers were encouraged to drive close to their driving style to minimize the bias in the operating speeds between instrumented and noninstrumented vehicles.

Most prior studies followed a similar approach to analyze the operating speed data and develop operating speed profile models (Wang et al. 2006; Memon et al. 2008; Montella et al. 2014b; Hashim et al. 2016; Wang et al. 2018; Malaghan et al. 2020a, b, 2021a, b). Further, studies found no significant difference in the operating speeds between instrumented and noninstrumented vehicles (Pérez Zuriaga et al. 2010; Pérez-Zuriaga et al. 2013). The data collection extended for 6 months, and the total time spent was 126 person-h.

Table 3. Description of the sections for data extraction on the road segments

Sections	Description
1-1	Beginning of the approach tangent
2-2	End of the approach tangent/point of curvature
3-3	Point of tangency/beginning of the departure tangent
4-4	End of the departure tangent

Data Extraction and Reduction

The speed data recorded at 10 Hz along the trajectory of the selected road sections were used to draw the operating speed profiles for the horizontal curves. Each of the selected road segments was subdivided into tangents and curves by referencing the position coordinates (latitude and longitude) at the beginning and end of the tangents and curves, respectively [Fig. 2(a) and Table 3].

Fig. 2(a) is a schematic representation of the geometric elements in the direction of travel as the vehicle traverses from Section 1-1 to Section 4-4. Section 1-1 to Section 2-2 represents the approach tangent, Section 2-2 to Section 3-3 represents a horizontal curve, and Section 3-3 to Section 4-4 represents the departure tangent [Fig. 2(a) and Table 3]. The speed data corresponding to the distance at 0.1 s along the horizontal curve were extracted by referencing the position coordinates at Section 2-2 (beginning of the curve) and Section 3-3 (end of the curve) [Figs. 2(a and b) and Table 3]. The data obtained were used to plot the operating speed profiles on the horizontal curves. A typical operating speed profile for a given curve features is shown in Fig. 2(b). In total, 3,798 speed profiles on the horizontal curves were extracted for the analysis. The data extraction and plotting of the profiles were performed using code developed in R Studio 3.6.0.

Several studies recommended a time headway between the host vehicle and following vehicle ranging from 4 to 6 s to ensure the influence of road geometry on the operating speed (Fitzpatrick et al. 2000; Malaghan et al. 2021b). In this study, the instrumented vehicle was not equipped with the headway measurement device to determine the minimum gap between the subject vehicle (instrumented vehicle) and the lead vehicle. Hence, headway data at specific intervals along the horizontal curves were not available. This study ensured the influence of the road geometry on operating speed by visually inspecting the patterns in the operating speed profiles along the horizontal curves and presence/absence of lead vehicle using video data. After visual inspection of the operating speed profiles and vedio data, the profiles showing abnormal variation, i.e., without any defined patterns due to the vehicular interaction (for example, presence of lead vehicle) were removed from the analysis.

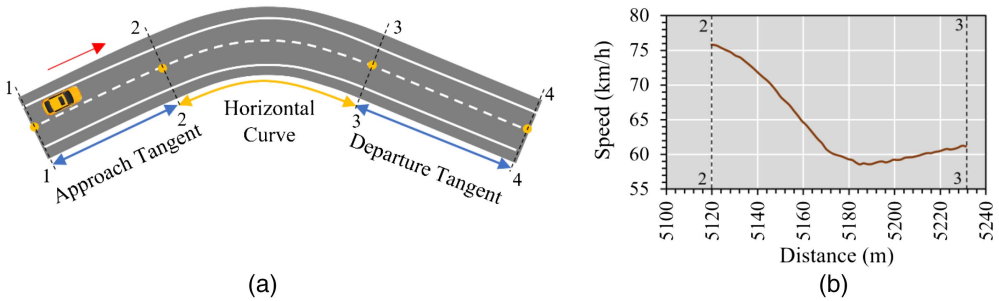

Fig. 2. (a) Operating speed profile for the horizontal curve; and (b) representation of the geometric elements.

J. Transp. Eng., Part A: Systems, 2023, 149(2): 04022151

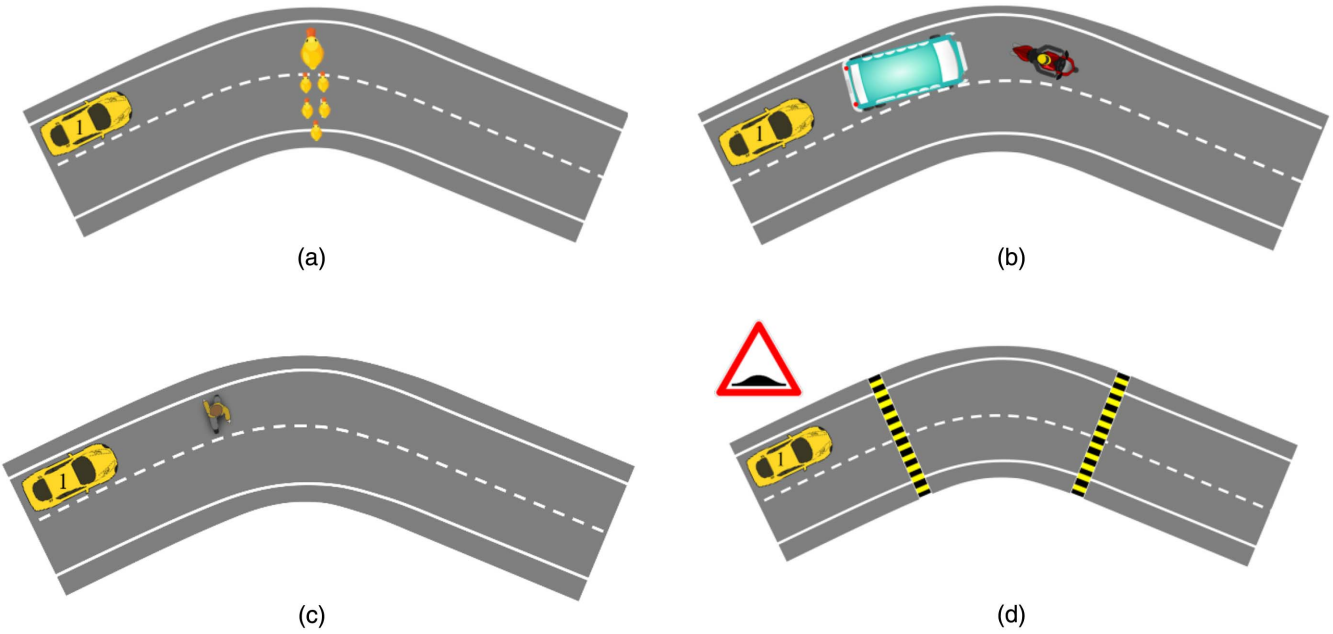

Fig. 3. Influence of the random events on the operating speed other than road geometry: (a) animals crossing; (b) vehicular interaction; (c) pedestrian crossing; and (d) speed bump at the curve entry and end.

From the visual inspection of patterns and vedio data, it was possible to manually remove the speed profiles that were influenced by following the lead vehicle too closely. In addition, if the following vehicle was far (>5 s) from the lead vehicle (based on visual inspection), the time headway was determined using vedio data by referencing fixed objects along the side of the curves in the surrounding road environment. However, due to low traffic volume as observed during site visit and data collection, it was possible to obtain most of the operating speed profiles without the presence of lead vehicle that might influence the variation in the patterns of the operating speed profiles.

In this study, the influence of factors on the operating speed of the host vehicle due to the random events other than road geometry such as sudden entry of the birds/animals [Fig. 3(a)], vehicular interactions [Fig. 3(b)], crossing pedestrians [Fig. 3(c)], and presence of speed humps at the PC and PT [Fig. 3(d)] were removed from the analysis by visualizing the patterns and vedio data. Also, data lost due to the sudden loss of GPS signal were removed from the analysis. Hence, a total of 854 operating speed profiles affected alone by road geometry from 13 horizontal curves (Table 4) out of 49 curves along the total length of 8,200 m of the selected road sections were considered in further analysis.

Clustering

Clustering is an unsupervised machine learning approach used to partition the observations into different groups so that observations in a group are quite similar to each other. In contrast, the observations in different groups are quite different from each other (Gareth et al. 2013). In this study, a *k*-means clustering approach was used to partition the data into *k* different sets. The observations are partitioned in to *k* clusters such that the total within-cluster variation added over all *k* clusters is minimized. The most common choice to define the within-cluster variation involves squared Euclidean distance. The *k*-means clustering approach was used to understand if the operating speed profiles on the horizontal curves followed a defined pattern or set of patterns.

The optimal number of clusters was determined using four methods: elbow method, silhouette method, gap statistic method, and using the NbClust function (Kabacoff 2011). The fourth method using the NbClust () function computes the optimal number of clusters for each of the 30 indices. The 30 indices are Calinski-Harabasz (CH) index, Duda index, Pseudot2 index, C-index, Gamma index, Beale index, cubic clustering criterion, PtBiserial index, Gplus index, Davies-Bouldin (DB) index, Frey index, Hartigan index, Tau index, Ratkowsky index, Scott index, Marriot

Table 4. Number of operating speed profiles considered in the analysis for the selected horizontal curves

Geometric features	Number of operating speed profiles		Geometric features	Number of operating speed profiles	
	Collected	In analysis		Collected	Analysis
$R = 60$, $L_c = 50$	87	73	$R = 150$, $L_c = 65$	87	54
$R = 80$, $L_c = 60$	87	72	$R = 150$, $L_c = 105$	91	72
$R = 80$, $L_c = 87$	87	64	$R = 170$, $L_c = 107$	91	64
$R = 90$, $L_c = 64$	91	58	$R = 200$, $L_c = 64$	91	59
$R = 95$, $L_c = 47$	87	72	$R = 200$, $L_c = 105$	91	72
$R = 100$, $L_c = 70$	87	57	$R = 300$, $L_c = 126$	91	64
$R = 130$, $L_c = 62$	91	73	—	—	—

Note: Curve radius (R) and curve length (L_c) are in meters.

J. Transp. Eng., Part A: Systems, 2023, 149(2): 04022151

index, Ball index, TraceCovW (Trace of the within clusters pooled covariance matrix) index, TraceW index, Friedman index, McClain index, Rubin index, Krzanowski-Lai (KL) index, Silhouette index, Gap index, Dindex, Dunn index, Hubert index, SDbw (average scattering for clusters and density between clusters) and SDindex.

Analysis of Operating Speed Profiles on Horizontal Curves

The operating speed profiles on the 13 horizontal curves with different geometric features were analyzed to identify the patterns in the operating speed profiles. This study identified and considered five primary operating speed profile variables, namely operating speed at PC (V_{PC}), operating speed at PT (V_{PT}), minimum operating speed on the curve (V_{cmin}), deceleration length on the curve (D_{cl}), and acceleration length on the curve (A_{cl}), to cluster the operating speed profiles with a similar pattern.

The cluster analysis was performed separately on the variables in the operating speed profiles for each of the 13 horizontal curves having different geometric design features. The results of the summary statistics of the acceleration and deceleration lengths of the operating speed profiles for the respective clusters in each of the 13 curve sites is presented in Table 5. Of 41 clusters of different curve sites, nine clusters showed deceleration ending before the MC and eight clusters showed deceleration ending after the MC. The percentage of the operating speed profiles in each cluster that attained deceleration end before and after the MC is presented in Table 5.

To begin with, for Curve site 1 (CS1) having a curve radius of 60 m and curve length of 50 m, the operating speed profiles on this horizontal curve were clustered into three groups (Fig. 4 and Table 5). The silhouette and gap statistic methods computed the optimal number of clusters as four and one, respectively [Figs. 4(a and b)]. The location on the knee in the elbow method suggested the optimal number of clusters as three [Fig. 4(c)]. The fourth method using NbClust () function computed the optimal number of clusters for each of the 30 indices.

For example, one of the indices is a Dindex, and the plots are shown in Fig. 4(d). The significant knee in the Dindex can be obtained from the significant peak in the second differences Dindex plot [Fig. 4(d)] that corresponds to a significant increase in the value of this index. The Dindex proposed an optimal number of clusters as four. Out of 30 indices, four indices proposed two as the optimal number of clusters, seven proposed three as the optimal number of clusters, three proposed five as the optimal number of clusters, one proposed seven as the optimal number of clusters, one proposed 10 as the optimal number of clusters, three proposed 11 as the optimal number of clusters, one proposed 14 as the optimal number of clusters, and three proposed 15 as the optimal number of clusters. The optimal number of clusters is three, as per the majority rule from all the four methods, as shown in the frequency histogram [Fig. 4(e)]. Therefore, the optimal number of clusters is three for CS1. For CS1, the percentage of operating speed profiles in Clusters 1, 2, and 3 are 20%, 41%, and 39%, respectively (Table 5).

Several studies assumed the occurrence of a minimum operating speed or the end of the deceleration at the midpoint of the curve (Jacob and Anjaneyulu 2013; Sil et al. 2020). In other words, the deceleration and acceleration lengths were assumed to be approximately equal, and the operating speed profile to be symmetric around the MC (Figueroa Medina and Tarko 2007). Hence, the percentage of operating speed profiles ending the deceleration before and after the MC for each cluster in different curve sites are presented in Table 5. All the operating speed profiles ended deceleration after the MC in Cluster 1 for CS1. The average percentage

Table 5. Summary statistics of the operating speed profiles in different clusters for the curves with different geometric features

CS	GF	Cluster	Deceleration length (m)				Acceleration length (m)				Average percentage length		Percentage of speed profiles	Speed profiles ending deceleration before and after MC (%)	
			Minimum	Maximum	Mean	SD	Minimum	Maximum	Mean	SD	D	A	Group	Before MC	After MC
CS1	$R = 60$, $L_c = 50$	1	28.825	49.715	40.404	5.757	1.265	29.884	7.442	7.551	85.087	14.913	1	0.000	100.00
		2	25.880	51.875	36.997	7.074	0.125	25.361	13.449	7.457	73.535	26.465	1	3.703	96.296
		3	1.347	24.538	12.926	6.907	24.997	50.509	37.232	6.413	25.532	74.468	2	100.000	0.000
CS2	$R = 80$, $L_c = 60$	1	34.060	57.127	47.753	9.870	5.182	20.905	11.697	7.245	79.886	20.114	1	0.000	100.000
		2	32.059	48.594	37.996	4.899	9.279	25.967	19.676	4.981	65.905	34.095	1	0.000	100.000
		3	14.260	33.694	21.966	5.153	25.222	43.085	34.851	5.025	38.628	61.372	2	94.737	5.263
		4	8.459	29.049	20.035	5.696	29.815	47.536	36.922	5.437	35.122	64.878	2	100.000	0.000
CS3	$R = 80$, $L_c = 87$	1	49.193	80.000	63.034	8.282	1.530	35.528	21.131	8.439	74.926	25.074	1	0.000	100.000
		2	19.090	56.044	39.646	9.012	27.671	64.342	46.355	9.065	46.105	53.895	3	65.385	34.615
		3	12.300	50.552	32.079	13.438	32.776	73.208	53.642	13.784	37.479	62.521	2	72.727	27.272
CS4	$R = 90$, $L_c = 64$	1	41.105	63.651	56.636	8.536	0.000	22.422	6.192	8.899	90.228	9.772	1	0.000	100.000
		2	16.063	38.558	29.236	6.394	24.904	47.120	33.950	6.297	46.252	53.748	3	66.667	33.333
		3	5.104	48.134	31.077	9.712	16.136	60.124	32.369	9.751	48.992	51.008	3	51.282	48.718

Table 5. (*Continued*.)

CS	GF	Cluster	Deceleration length (m)				Acceleration length (m)				Average percentage length		Group	Percentage of speed profiles	Speed profiles ending deceleration before and after MC (%)	
			Minimum	Maximum	Mean	SD	Minimum	Maximum	Mean	SD	*D*	*A*			Before MC	After MC
CS5	$R = 95$,	1	23.048	46.463	32.128	6.200	0.597	26.106	15.013	6.710	68.330	31.670	1	27.143	5.263	94.737
	$L_c = 47$	2	0.779	28.708	16.001	7.498	17.097	46.281	31.248	7.610	33.892	66.108	2	44.286	87.097	12.903
		3	1.371	25.004	12.986	6.183	22.727	44.431	34.505	6.202	27.325	72.675	2	28.571	90.000	10.000
CS6	$R = 100$,	1	36.767	69.057	48.526	7.688	0.000	35.615	23.229	8.152	67.703	32.297	1	32.143	0.000	100.000
	$L_c = 70$	2	18.929	71.074	44.796	15.869	0.000	51.203	26.762	15.556	62.511	37.489	1	33.929	26.316	73.684
		3	0.000	38.102	23.252	10.515	34.338	72.572	48.304	10.723	32.533	67.467	2	33.929	94.737	5.263
CS7	$R = 130$,	1	5.435	57.924	33.142	10.876	3.687	53.500	25.633	10.278	56.226	43.774	4	61.290	36.842	63.160
	$L_c = 62$	2	2.989	38.988	26.537	8.996	17.391	58.787	31.676	10.464	45.979	54.021	3	38.710	54.167	45.833
CS8	$R = 150$,	1	39.899	66.433	56.427	9.870	0.000	25.208	9.661	9.607	85.334	14.666	1	18.000	0.000	100.000
	$L_c = 65$	2	5.203	35.805	23.334	10.212	28.193	62.222	42.892	10.307	35.251	64.749	2	32.000	81.250	18.750
		3	0.000	45.929	18.664	13.290	20.960	65.937	47.039	12.999	28.171	71.829	2	50.000	92.000	8.000
CS9	$R = 150$,	1	57.069	103.425	76.049	15.185	2.355	48.095	32.127	17.795	70.719	29.281	1	26.230	0.000	100.000
	$L_c = 105$	2	30.911	76.806	55.020	9.762	29.776	72.277	49.519	9.741	52.635	47.366	4	52.459	40.625	59.375
		3	35.607	65.553	48.479	9.049	48.963	83.711	63.269	10.308	43.433	56.567	3	21.312	76.923	23.077
CS10	$R = 170$,	1	41.785	85.341	59.545	9.281	15.337	61.498	46.052	9.868	56.457	43.543	4	53.448	22.581	77.419
	$L_c = 107$	2	52.354	92.195	65.285	8.950	17.643	59.843	41.566	10.089	61.219	38.781	1	31.035	5.556	94.444
		3	17.268	50.785	34.606	11.567	57.083	87.673	71.430	9.745	32.448	67.552	2	15.517	100.000	0.000
CS11	$R = 200$,	1	20.74	57.396	35.027	10.672	1.949	41.384	25.434	12.294	58.478	41.523	4	37.879	48.000	52.000
	$L_c = 64$	2	0.000	31.019	15.390	10.123	27.655	65.000	45.493	11.161	25.496	74.504	2	18.182	100.000	0.000
		3	3.805	23.432	12.080	6.512	37.804	60.513	48.681	7.539	19.985	80.015	2	27.758	100.000	0.000
CS12	$R = 200$,	1	56.964	97.114	80.172	14.618	1.726	43.675	20.372	15.838	79.92	20.08	1	10.448	0.000	100.000
	$L_c = 105$	2	43.328	80.231	61.965	12.332	18.895	55.486	40.068	12.731	60.787	39.213	1	11.940	25.000	75.000
		3	36.999	65.873	51.110	8.891	33.566	69.489	53.102	9.797	49.118	50.882	3	31.343	57.143	42.857
		4	3.255	40.128	26.601	9.203	63.941	108.171	78.861	10.398	25.273	74.727	2	25.373	100.000	0.000
		5	0.000	30.803	12.731	11.513	74.747	105.000	93.549	10.813	11.904	88.096	2	19.403	100.000	0.000
CS13	$R = 300$,	1	14.000	98.659	66.316	18.675	18.112	109.644	54.900	19.432	54.807	45.193	3	37.735	40.000	60.000
	$L_c = 126$	2	1.376	50.373	22.243	14.076	42.222	125.260	100.195	19.147	18.540	81.460	2	62.264	0.000	100.000

Note: CS = curve site; CS1, CS2, . . . , CS13 = Curve site 1, Curve site 2, ..., Curve site 13; GF = geometric features; *D* = deceleration; *A* =acceleration; and MC = midpoint of curve.

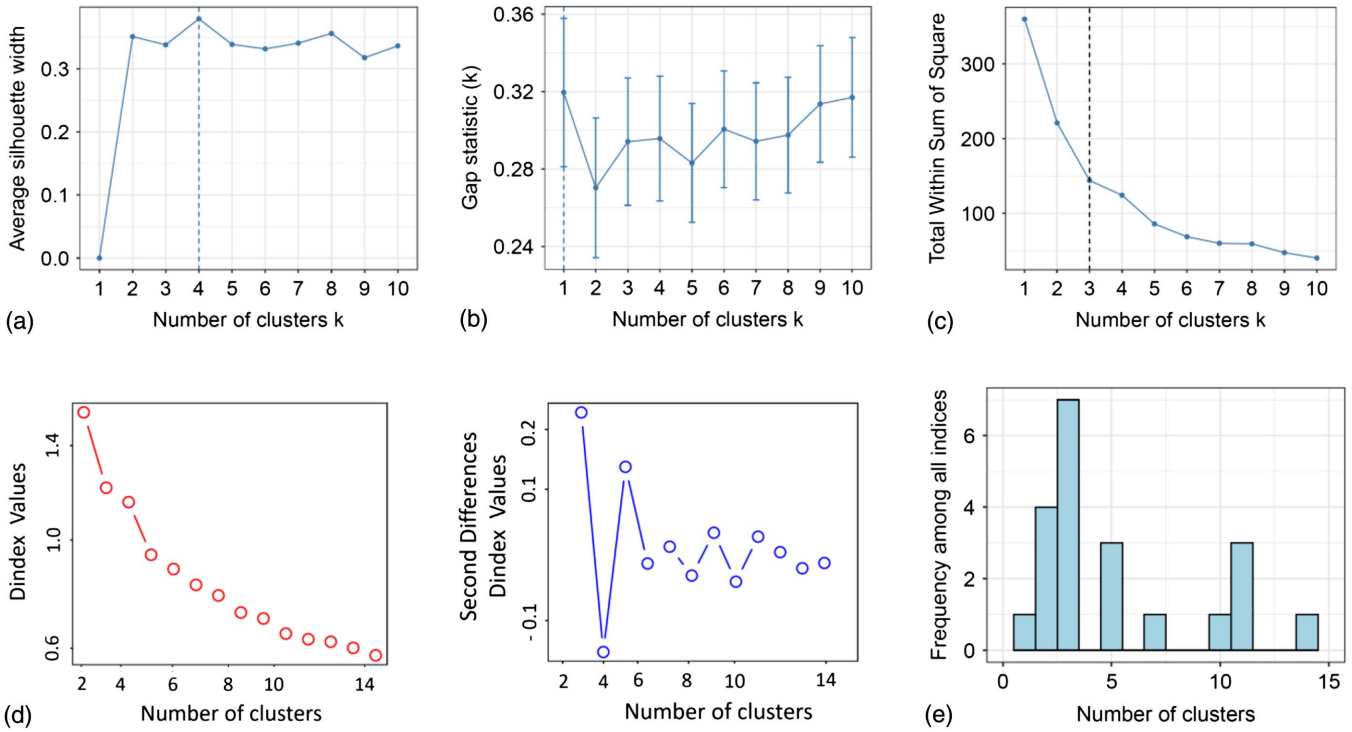

Fig. 4. Four methods showing the optimum number of clusters: (a) silhouette method; (b) gap statistic method; (c) elbow method; (d) NbClust function; and (e) frequency histogram.

deceleration length on the curve is 85%, and the average percentage acceleration length was 15% for the operating speed profiles in Cluster 1 for the CS1.

The pattern of the operating speed profiles in Curve site 1 for Cluster 1 (CS1-C1) is shown in Fig. 5. Here, CS1 indicates the curve site number, which is one in this case, and C1 indicates the cluster number, which is also one in this case. These notations are followed and presented further to identify the curve number and cluster number as presented in the top left corner for each cluster in Fig. 5. The operating speed profiles in CS1-C1 show a continuous decrease in operating speed from PC with a steep slope followed by a constant operating speed or marginal increase in the operating speed until the PT. Overall, this variation in the operating speed is represented by the average operating speed profile shown in the ldashed line (Fig. 5).

In the case of CS1-C2, 96% of the operating speed profiles ended deceleration before the MC and the remaining 4% after the MC (Fig. 5 and Table 5). The average percentage deceleration and acceleration lengths were 74% and 26%, respectively. The operating speed values decreased continuously with a steeper slope, followed by a constant or mild slope with a marginal increase in the operating speed values. This variation in the operating speed values for the operating speed profiles in Cluster 2 is shown by an average operating profile (dashed line in Fig. 5).

In the case of CS1-C3, the operating speed profiles showed a decrement in the speed values near PC for a smaller distance followed by an increase in the operating speed values continuously until the PT (Fig. 5). The average percentage deceleration length of the operating speed profiles in this cluster was 25%, and the average percentage acceleration length was 75% (Table 5). All the operating speed profiles showed the end of deceleration before the MC, and the drivers began the acceleration before the MC, which is continued until PT.

For Curve site 2 ($R = 80$ m and $L_c = 60$ m), the operating speed profiles in Cluster 1 are fewer in number, and a definite pattern could not be observed from this cluster (Fig. 5). However, the operating speed profiles showed complete deceleration on the curve. In Cluster 2, the operating speed profiles showed a decrement in the speed over major section of the curve from PC and then an increase in the speed until the curve end (Fig. 5). In Clusters 3 and 4, the pattern of the operating speed profiles was similar, i.e., the driver decelerated initially after entering the curve and after that, accelerated in the major part of the curve (Fig. 5). However, the average percentage of deceleration length (39%) in the operating speed profiles in Cluster 3 was higher than that in Cluster 4 (35%) (Table 5). In Clusters 1 and 2, all the operating speed profiles ended deceleration after the MC, whereas all the operating speed profiles ended deceleration before MC in Cluster 4. In the case of Cluster 3, 95% of the operating speed profiles ended deceleration after the MC, and the remaining did so before the MC (Table 5). Table 6 provides the explanation for the patterns in the operating speed profiles in each cluster for the rest of the horizontal curves with different geometric features.

One-way ANOVA testing was conducted to check if any statistically significant difference existed in the means of the deceleration and acceleration lengths of the operating speed profiles in each cluster for thirteen different horizontal curves, with the following hypotheses:

- Null hypothesis: the means of the deceleration and acceleration lengths in a cluster are the same.
- Alternative hypothesis: the means of the deceleration and acceleration lengths are different in a cluster.

The results of the ANOVA test are presented for the deceleration and acceleration lengths in each cluster for 13 curves with different geometric design features in Table 7.

From Table 7, it can be seen that the means of the deceleration and acceleration lengths for the operating speed profiles in 34 clusters were statistically different at a 0.05 significance level. Thus, the test rejected the null hypothesis stating that the means

of the deceleration and acceleration lengths are the same in the operating speed profiles for 85% of the clusters. However, it can be seen from the results of Table 7 (in bold) that the means of the deceleration and acceleration lengths for the operating speed profiles in each of the six clusters are not statistically different at a 0.05 significance level. Thus, the test failed to reject the null hypothesis that the means of the deceleration and acceleration lengths are the same in the operating speed profiles for 15% of the clusters. Therefore, assuming equal acceleration and deceleration lengths to measure the minimum operating speed at the midpoint of the curve is not appropriate in the majority of the operating speed profiles.

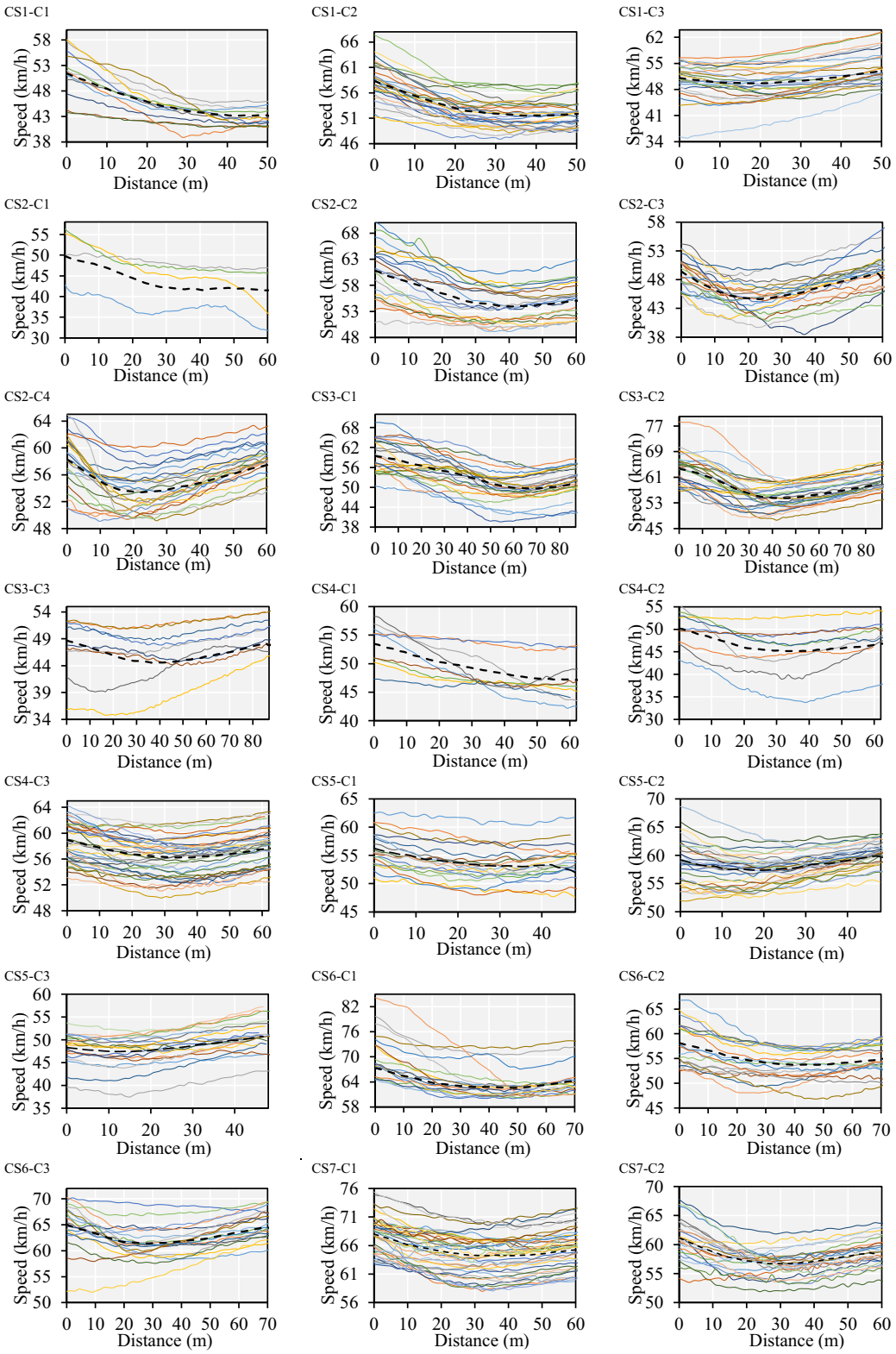

Fig. 5. Clusters showing the patterns of the operating speed profiles for different curves.

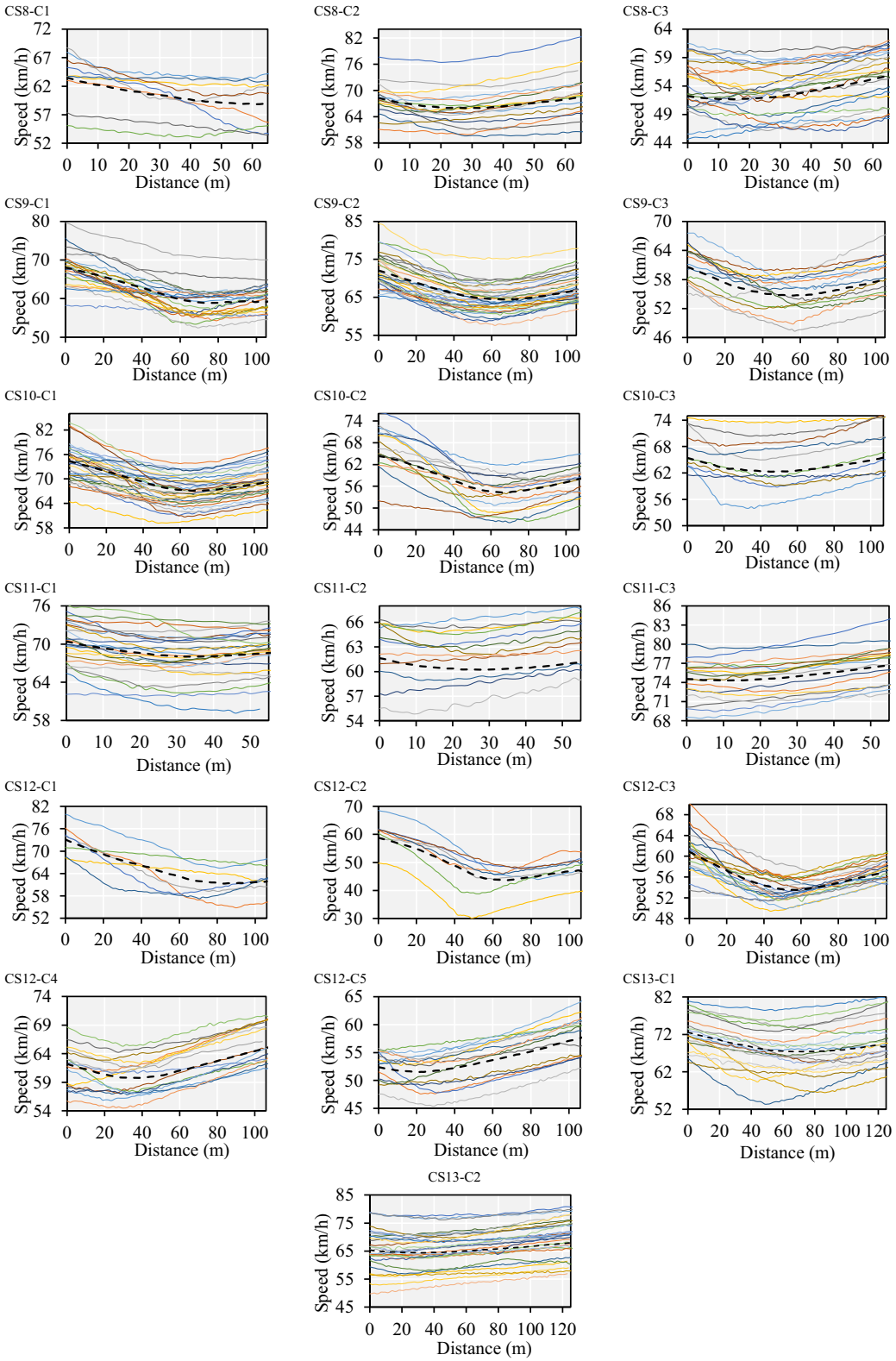

Fig. 5. (*Continued.*)

Grouping of Patterns in the Operating Speed Profiles on Horizontal Curves

The group of operating speed profiles in each cluster represents a pattern. Further, the patterns of the operating speed profiles in different clusters of different curve sites were observed to be similar. Hence, this study grouped the clusters of operating speed profiles with a similar pattern. All 40 clusters were grouped into four generalized patterns, and the discussion is presented in the following subsections.

Table 6. Explanation for the pattern of operating speed profiles in each cluster for different curve sites

Curve site	Remarks
CS3	For Curve site 3 ($R = 80$ m and $L_c = 87$ m), the operating speed profiles in Cluster 1 showed that drivers decelerate in the major portion of the curve length from PC, followed by acceleration in the minor portion of the curve length until PT (Fig. 5). The average percentage acceleration and deceleration lengths are 25% and 75%, respectively (Table 5). In the case of Cluster 2, the average percentage deceleration and acceleration lengths are 46% and 54%, respectively. The average acceleration length (54 m) is slightly higher than the average deceleration length (46 m), and the positions of minimum operating speeds in the operating profiles are located near the MC (Fig. 5). In Cluster 3, the number of operating speed profiles is lower, and a defined pattern of the operating speed profiles was not observed. However, the major part of the curve length is traversed in acceleration.
CS4	For Curve site 4 ($R = 80$ m and $L_c = 87$ m), the number of operating speed profiles was lower than in Clusters 1 and 2. A defined pattern of operating speed profiles was not observed in Cluster 2; however, most of the operating speed profiles in Cluster 1 showed a complete deceleration with a steeper slope (Fig. 5). In Cluster 3, the average percentage deceleration and acceleration lengths are 49% and 51%, respectively. The average acceleration length (32 m) of the operating speed profiles is marginally greater than the deceleration length (31 m). The cluster of the operating speed profiles was observed to be approximately symmetric around the MC (Fig. 5).
CS5	For Curve site 5 ($R = 95$ m and $L_c = 47$ m), the operating speed profiles in Cluster 1 showed that the major portion of the curve is traversed in deceleration with a mild slope in both acceleration and deceleration (Fig. 5). The average percentage deceleration and acceleration lengths are 68% and 32%, respectively. Clusters 2 and 3 showed a similar pattern, i.e., a smaller portion of the curve is traversed in deceleration from PC and a major portion of the curve traversed in acceleration (Fig. 5). However, the average deceleration length (16 m) in Cluster 2 is higher than the average deceleration length (13 m) in Cluster 3 (Table 5). The percentage deceleration lengths in Clusters 2 and 3 are 34% and 27%, respectively, whereas, the average acceleration lengths in the Clusters 2 and 3 are 66% and 73%, respectively.
CS6	For Curve site 6 ($R = 100$ m and $L_c = 70$ m), Clusters 1 and 2 showed similar patterns, i.e., the drivers decelerate after entering the curve for major distance on the curve and then accelerate until the curve end (Fig. 5). The first two clusters showed a difference in the average lengths of the deceleration in the descending order (68% in C1 and 66% in C2) (Table 5). The average deceleration lengths in C1 and C2 are 49 and 45 m, respectively, whereas, the average acceleration lengths in C1 and C2 are 23 and 27 m, respectively. In the third cluster, the drivers decelerate for a shorter distance after entering the curve and accelerate for a major distance until the curve ends (Fig. 5). The percentage average deceleration and acceleration lengths in C3 are 33% and 68%, respectively.
CS7	For Curve site 7 ($R = 130$ m and $L_c = 62$ m), the pattern of the operating speed profiles appear to be approximately symmetric about the MC in Cluster 1 (Fig. 5). The average percentage deceleration and acceleration lengths in C1 are 56% and 43%, respectively. The average percentage deceleration length (33 m) is higher than the average percentage acceleration length (26 m), and the majority of the operating speed profiles (63%) end the deceleration after the MC (Table 5). In contrast, in Cluster 2, the average percentage deceleration length (45%) is lower than the average percentage acceleration length (54%) and the majority of the operating speed profiles ended the deceleration (54%) after the MC (Fig. 5).
CS8	For Curve site 8 ($R = 150$ m and $L_c = 65$ m), most of the operating speed profiles showed deceleration with a steeper slope on the major portion of the curve, followed by a constant or marginal increase in the operating speed until the curve end (Fig. 5). The operating speed profiles in Cluster 2 are characterized by average deceleration lengths (23 m) smaller than the average acceleration length (43 m) with a mild slope in deceleration and steeper slope in acceleration (Fig. 5 and Table 5). In Cluster 3, the operating speed profiles show a major portion in acceleration (72%) with steeper slopes in the profiles (Fig. 5 and Table 5).
CS9	For Curve site 9 ($R = 150$ m and $L_c = 105$ m), the operating speed profiles showed a greater deceleration length (71%) followed by an acceleration length (30%) for a shorter distance in Cluster 1 (Fig. 5), whereas in Cluster 2, the pattern of the operating speed profiles was observed to be symmetric about the MC. The average percentage deceleration (53%) is slightly higher than the average percentage acceleration length (47%) and the majority of the operating speed profiles complete the deceleration after the MC (Fig. 5 and Table 5). In contrast, the operating speed profiles in Cluster 3 showed a lower average length of deceleration (49 m) than the length of the acceleration (64 m) (Fig. 5 and Table 5).
CS10	For Curve site 10 ($R = 170$ m and $L_c = 107$ m), the pattern in Cluster 1 is similar to that in Cluster 2 for Curve site 9 (CS9-C2) (Fig. 5). The pattern in Cluster 2 for Curve site 10 (Fig. 5) is similar to that in Cluster 1 of CS9; however, the average percentage deceleration length is greater in CS9-C1 (70%) than that in CS10-C2 (61%). In Cluster 3, the number of operating speed profiles is lower; a defined pattern in the operating speed profile could not be observed.
CS11	For Curve site 11 ($R = 200$ m and $L_c = 64$ m), the operating speed profiles showed mild slope in deceleration and acceleration, and the average percentage length of the deceleration (59%) is higher than the average percentage length of the acceleration (42%) in Cluster 1 (Fig. 5 and Table 5). The operating speed profiles in Clusters 2 and 3 showed a similar pattern with acceleration length (80%) in C3 higher than the acceleration length (75%) in C2 (Fig. 5 and Table 5).
CS12	For Curve site 12 ($R = 200$ m and $L_c = 105$ m), the pattern in the operating speed profile for Cluster 1 (Fig. 5) was similar to the pattern in the operating speed profiles in CS1-C1, CS2-C1, CS4-C1, and CS8-C1. The pattern of the operating speed profiles in Clusters 2 and 3 are similar; however, the deceleration length (61%) in Cluster 2 is higher than the deceleration length (49%) in Cluster 3 (Fig. 5 and Table 5). Similarly, the pattern of the operating speed profiles in Clusters 4 and 5 are similar, with the major portion of the curve traversed in acceleration with a steeper slope in the speed profiles (Fig. 5 and Table 5). The percentage acceleration length (8%) in C5 is higher than that in the C4 (75%).
CS13	For Curve site 13 ($R = 300$ m and $L_c = 126$ m), the pattern in the operating speed profiles for C1 is not clear. However, the operating speed profiles are characterized by the deceleration length (55%) higher than the acceleration length (45%) (Fig. 5). In Cluster 2, the deceleration length (18%) is lower with marginal variation in the operating speed followed by an increase in the operating speed with the major portion of the curve traversed in acceleration (82%) (Fig. 5).

Note: CS = curve site.

Table 7. Summary of the ANOVA results for deceleration and acceleration lengths of operating speed profiles in each cluster for curves with different design features

Serial number	Geometric features	Cluster No.	F-value	p-value	F-critical
1	$R = 60$,	1	156.672	<0.001	4.260
	$L_c = 50$	2	141.710	<0.001	4.027
		3	172.919	<0.001	4.034
2	$R = 80$,	1	52.031	<0.001	4.965
	$L_c = 62$	2	144.401	<0.001	4.085
		3	60.885	<0.001	4.113
		4	105.778	<0.001	4.062
3	$R = 80$,	1	313.969	<0.001	4.043
	$L_c = 87$	2	7.161	0.010	4.034
		3	13.802	0.001	4.351
4	$R = 90$,	1	150.620	<0.001	4.494
	$L_c = 64$	**2**	**2.483**	**0.135**	**4.494**
		3	**0.343**	**0.559**	**3.967**
5	$R = 95$,	1	66.674	<0.001	4.113
	$L_c = 47$	2	63.134	<0.001	4.001
		3	120.739	<0.001	4.098
6	$R = 100$,	1	101.993	<0.001	4.113
	$L_c = 72$	2	52.865	<0.001	4.113
		3	12.513	<0.001	4.113
7	$R = 130$,	1	9.567	0.003	3.970
	$L_c = 62$	**2**	**3.329**	**0.075**	**4.052**
8	$R = 150$,	1	103.751	<0.001	4.494
	$L_c = 65$	2	29.073	<0.001	4.171
		3	59.692	<0.001	4.043
9	$R = 150$,	1	56.400	<0.001	4.171
	$L_c = 105$	2	5.091	0.028	3.996
		3	15.114	<0.001	4.260
10	$R = 170$,	1	30.752	<0.001	4.001
	$L_c = 107$	2	55.671	<0.001	4.130
		3	53.349	<0.001	4.494
11	$R = 200$,	1	8.680	0.005	4.043
	$L_c = 64$	2	47.897	<0.001	4.301
		3	**0.954**	**0.336**	**4.149**
12	$R = 200$,	1	53.890	<0.001	4.747
	$L_c = 105$	2	12.210	0.004	4.600
		3	**0.476**	**0.494**	**4.085**
		4	240.810	<0.001	4.149
		5	340.367	<0.001	4.260
13	$R = 300$,	1	355.069	<0.001	3.990
	$L_c = 126$	**2**	**3.588**	**0.066**	**4.098**

Group 1: Major Section of the Curve Length Traversed in Deceleration Followed by a Shorter Section of the Curve Length in Acceleration

In this group, the operating speed profiles are characterized by longer deceleration lengths and shorter acceleration lengths [Fig. 6(a)]. Out of 40 clusters, the operating speed profiles in 14 clusters (Table 5) showed an approximately similar pattern as shown in Fig. 6(a) and hence are categorized in Group 1. The drivers underwent deceleration for a longer distance after entering the curve; the average percentage deceleration length on the curves ranged from 61% to 90%. The deceleration was followed by a shorter acceleration length with a marginal increase in the operating speed when exiting the curve; the average percentage acceleration length on the curves ranged from 10% to 39%. Fewer operating speed profiles showed continuous deceleration from the PC to PT on the horizontal curves in these clusters [Fig. 6(c)].

Group 2: Shorter Section of the Curve Length in Deceleration Followed by a Major Section of the Curve Length in Acceleration

The generalized pattern of the operating speed profiles in this group was opposite to the pattern observed in Group 1. The pattern was characterized by shorter deceleration and longer acceleration lengths on the horizontal curve [Fig. 6(b)]. In total, the operating speed profiles in 14 clusters approximately showed this type of pattern and hence are categorized in Group 2. The average percentage deceleration length ranged from 12% to 39%, whereas the average percentage acceleration length ranged from 61% to 88%. It can also be observed that the range of percentage deceleration length (12% to 39%) in this group overlapped the percentage acceleration length (10% to 39%) with a marginal difference in Group 1. Similarly, the difference in overlap for the acceleration length (61% to 88%) in this group with the deceleration length (61% to 90%) in Group 1 was marginal. The operating speed profiles in these clusters also showed continuous acceleration from the point of curve entry to the curve exit [Fig. 6(d)].

Group 3: Deceleration Length Is Slightly Shorter Than the Acceleration Length and Deceleration Ends before MC

In the third group, the pattern of operating speed profiles in the clusters were characterized by approximately similar deceleration and acceleration lengths [Fig. 6(e)]. However, the deceleration lengths were slightly lower than the acceleration lengths. This pattern was observed in the operating speed profiles in 7 of 40 clusters. The cluster of the speed profiles can be observed to be approximately symmetric about the MC. For example, this pattern can be clearly observed in Clusters 2 and 3 in Curve sites 3 and 4, respectively (Fig. 5). Most of the drivers ended the deceleration before MC; the average percentage deceleration and acceleration lengths ranged from 43% to 55% and 45% to 57%, respectively.

Group 4: Deceleration Length Is Slightly Greater Than the Acceleration Length and Deceleration Length Ends after MC

The generalized pattern of the operating speed profiles in this group was opposite to the pattern observed in Group 3. The pattern of the operating speed profiles observed in this group was characterized by deceleration lengths slightly greater than the acceleration length [Fig. 6(f)]. Of 40 clusters, the operating speed profiles in four clusters exhibited this type of pattern. Most of the drivers ended their deceleration after the MC, followed by an acceleration until the curve end. The average percentage deceleration length ranged from 53% to 58%, and the average acceleration length ranged from 42% to 47% (Table 5). The average percentage deceleration and acceleration lengths in this group overlapped the average percentage acceleration and deceleration lengths, respectively, in Group 3.

Discussion

This study used a clustering approach to investigate the patterns of the operating speed profiles on horizontal curves. Ottesen and Krammes (2000) and Fitzpatrick and Collins (2000) generalized the operating speed profiles on a tangent to curve and curve to

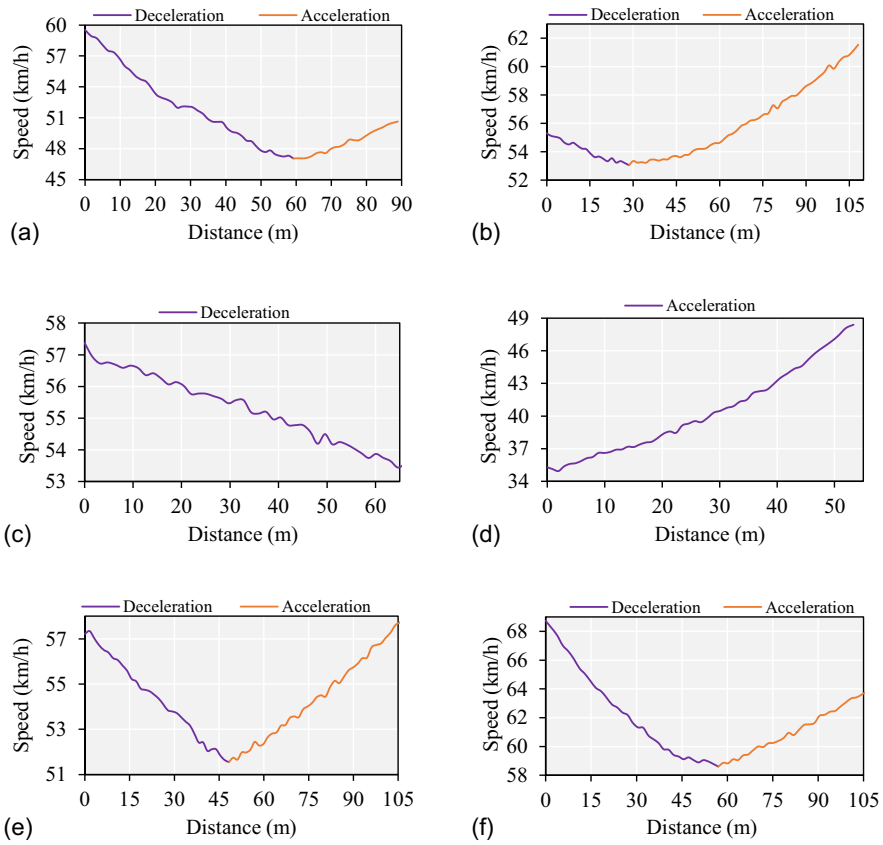

Fig. 6. Generalized patterns: (a) greater deceleration length; (b) greater acceleration length; (c) complete deceleration; (d) complete acceleration; (e) acceleration length marginally greater; and (f) deceleration length marginally greater.

tangent into three different cases. They assumed operating speed to be constant on the horizontal curves without any speed variation. On the other hand, several other studies approximated the acceleration and deceleration length to be equal and that the minimum operating speed occurred at the midpoint of the curve to model the geometric design consistency measures (Jacob and Anjaneyulu 2013; Sil et al. 2020; Figueroa Medina and Tarko 2007). The results from the clusters analysis of this study showed the variation in the operating speed on the horizontal curves with different patterns. The operating speed profiles in most of the clusters showed a major portion of the curve traversed in either acceleration or deceleration. Besides, the results of the ANOVA test showed that in 85% of the clusters, the mean lengths of acceleration and deceleration were found to be statistically different at a 5% significance level. Only in 15% of the clusters, the acceleration and deceleration lengths were approximately equal, and the minimum speed can be measured at the MC for such speed profiles.

A study by Malaghan et al. (2021a) analyzed the distribution of the positions of minimum operating speeds on the horizontal curves. On most of the horizontal curves, the minimum operating speed position data followed a normal distribution, with the frequency of the minimum operating speed positions decreasing from the MC toward the curve ends. These outcomes are consistent with the results from this study, because the numbers of operating speed profiles in the clusters falling in Groups 1 and 2 were lower. Although the study results by Malaghan et al. (2021a) presented the distribution of minimum speed positions on the horizontal curves, the patterns in the operating speed profile remained unexplored. Hence, this study determined the underlying patterns of the operating speed profiles leading to the occurrence of transition at a point where deceleration ends and acceleration commences on the horizontal curve.

Pérez Zuriaga et al. (2010) found that the average percentage deceleration length on the curve was 45% and that the deceleration ended before MC in 58% of the curve sites. Montella et al. (2014b) determined that in 27% of the transitions, the deceleration started before the MC, and in 63% of the transitions, the acceleration started after the MC. The most frequent pattern observed was the continuous deceleration in 22% of the transitions on the entire curve.

The aforementioned studies did not define any pattern in the operating speed profiles on the horizontal curve. Also, these studies presented the overall average results of the deceleration and acceleration maneuvers. In the present study, the patterns were clustered, and the descriptive statistics of the acceleration and deceleration maneuvers for each of the clusters showing similar patterns in the operating speed profiles are presented in Table 5.

Wang et al. (2020) observed six different patterns of the operating speed profiles on the curves sites located in the mountainous terrain: (1) continuous deceleration on the curve, (2) continuous acceleration on the curve, (3) deceleration followed by acceleration with minimum speed observed near the curve end, (4) deceleration followed by acceleration with minimum speed observed near the beginning of the curve, (5) deceleration followed by acceleration with the minimum speed observed near to the MC, and (6) successive deceleration and acceleration followed by deceleration without any defined pattern. These patterns are consistent with the patterns observed in this study except the sixth pattern. However, their study did not present the analysis results in grouping the operating speed profiles with a similar patterns.

Spacek (2005) studied the track behavior of the drivers along the curves in terms of speeds and classified the track paths into six types based on the test measurements. The six track types are ideal behavior, normal behavior, correcting, cutting, swinging, and drifting. The drivers attained the highest speeds on the curves by exhibiting cutting and swinging track types to compensate for the centrifugal acceleration when negotiating the curve. Also, a study by Fitzsimmions et al. (2013) found that the majority of the drivers exhibited a track type, which they called "cutting path" (centerline of the road cut by the vehicle path) and assumed that such behavior allowed the drivers to maintain greater speeds on the curves.

The lateral vehicle placement was found to increase with the decrease in the curve radius (Stodart and Donnell 2008; Ben-Bassat and Shinar 2011; Bella 2013). The trajectory of the vehicle profile was found to be significantly influenced by the travel direction (Stodart and Donnell 2008; Bella 2013), vehicle type (Fitzsimmons et al. 2013; Jacob and Violette 2012), speed, and lateral position at the beginning of the curve (Fitzsimmons et al. 2013). The lateral shift in the position was found to be greater in the case of heavy vehicles compared with passenger cars (Jacob and Violette 2012). Bella (2013) reported that drivers maintained higher speeds on curves with greater radii, and the lateral displacement was toward the curve center on left-hand curves and toward the right side on right-hand curves. The sharper the curve, the higher the lateral displacement. A study by Imran et al. (2006) found that the lateral displacement between the path followed and actual geometric alignment was high in the first half of the curve, with a marginal increase in the lateral position at the midpoint of the curve, which decreased as the vehicle traversed toward the curve end. Hence, in this study, the operating speed profiles clustered for different radii might not represent the ideal vehicle path, i.e., the vehicle path deviates more or less from the center of the lane.

Research Contribution

The maximum and minimum operating speeds on the tangents and curves, respectively, were measured to develop operating speed profile models to evaluate design consistency. Operating speed profile models are used to evaluate local and global design consistency. In local consistency evaluation, the design consistency of a geometric road elements are assessed, whereas in the global consistency, the design consistency of the entire road segment is assessed. For example, there is a direct correlation between operating speed difference between successive road geometric elements and crash rate on or near the horizontal curves (McFadden and Elefteriadou 2000). The thresholds based on the operating speed difference are established to classify the road geometric elements as poor, fair, and good; the geometric element that falls in the poor or fair category are considered to be inconsistent (Lamm et al. 1988). In global consistency evaluation, the global consistency models estimate crashes on the complete road section, considering the speed variation on the entire road segment (Llopis-Castelló et al. 2018b). The consistency parameter is determined by the operating speed and inertial operating speed profiles. Thus, the accurate measurement of minimum and maximum operating speed positions is required to develop the reliable operating speed profile models.

Hence, this study analyzed the patterns of the operating profiles on the horizontal curves. The insights of the study results help in a better understanding of the patterns of the operating speed profiles and, thereby, accurate measurement of the minimum operating speed and position on horizontal curves to promote the design consistency evaluation.

Summary and Conclusions

This study analyzed the patterns in the operating speed profiles on the horizontal curves of the rural roadway segments located in the plain terrain. The operating speed profiles were recorded on the selected road segments using a GPS device instrumented in passenger cars. The operating speed profiles between PC and PT were extracted for all the data samples for each curve site on each of the selected road sections. In total, the operating speed profiles on 13 horizontal curves were studied. The operating speed profiles on each curve were clustered separately using the k-means clustering approach. This study analyzed the patterns in the 40 clusters and categorized them into four groups. The key findings of the research study are as follows:

- Most of the clusters showed that the mean lengths of acceleration and deceleration were statistically different. This implies that measurement of operating speed at the end of deceleration resulted in accurate determination of minimum operating speed on the horizontal curve in evaluating design consistency. In others words, the deceleration end will not coincide with the MC in all the operating speed profiles; the measurement of the operating speed at MC might not result in the accurate measurement of minimum operating speed in design consistency evaluation.
- The primary patterns observed included (1) longer deceleration length followed by a marginal acceleration length for a shorter distance, (2) shorter deceleration length followed by longer acceleration length, (3) deceleration length slightly greater than acceleration length, and (4) deceleration length slightly shorter than the acceleration length. In addition to the four patterns, majority of the operating speed profiles in Groups 1 and 2 showed continuous acceleration and continuous deceleration between PC and PT. These results imply that the drivers exhibited set of defined patterns in the operating speed profiles on the horizontal curves. Thus, assuming a constant operating speed on the curve and approximating the acceleration and deceleration lengths to be equal is not true for all the operating speed profiles.
- The study did not observe any constant operating speed profiles without variation in the operating speed on the horizontal curves.

Limitations and Future Research Work

This study has a few limitations, which can be addressed in future research work, as follows:

- In this study, only the variation in the operating speed on horizontal curves was studied. Because the maximum operating speed on the tangent was measured in developing the operating speed profile models, the patterns in the operating speed profiles from tangent to curve and curve to tangent can be identified using the clustering approach.
- The study identified the patterns in the operating speed profiles on the curves sites located in plain terrain. It will be interesting to identify the patterns of the operating speed profiles in rolling and mountainous terrain along with a downgrade and upgrade on the selected road sections. In addition, the static and dynamic characteristics of the vehicle types influence the road geometry; the patterns in the operating speed profiles can be analyzed for different vehicle types for heterogeneous traffic conditions.
- This study obtained vehicle kinematics data only for professional male drivers. Further studies should obtain the data for different driver types (professional/nonprofessional drivers), including male and female drivers representing the entire driver population of the long-term naturalistic driving data to compare with the results presented in this study.

Data Availability Statement

Some or all data, models, or code that support the findings of this study are available from the corresponding author upon reasonable request.

References

AASTHO. 2011. *A policy on geometric design of highways and streets*. Washington, DC: AASHTO.

Bella, F. 2013. "Driver perception of roadside configurations on two-lane rural roads: Effects on speed and lateral placement." *Accid. Anal. Prev.* 50 (Jan): 251–262. https://doi.org/10.1016/j.aap.2012.04.015.

Bella, F. 2014. "Driver performance approaching and departing curves: Driving simulator study." *Traffic Inj. Prev.* 15 (3): 310–318. https://doi.org/10.1080/15389588.2013.813022.

Ben-Bassat, T., and D. Shinar. 2011. "Effect of shoulder width, guardrail and roadway geometry on driver perception and behavior." *Accid. Anal. Prev.* 43 (6): 2142–2152. https://doi.org/10.1016/j.aap.2011.06.004.

Camacho-Torregrosa, F. J., A. M. Pérez-Zuriaga, J. M. Campoy-Ungría, and A. García-García. 2013. "New geometric design consistency model based on operating speed profiles for road safety evaluation." *Accid. Anal. Prev.* 61 (Dec): 33–42. https://doi.org/10.1016/j.aap.2012.10.001.

Dhahir, B., and Y. Hassan. 2018. "Studying driving behaviour on horizontal curves using naturalistic driving study data." *Transp. Res. Rec.* 2672 (17): 83–95. https://doi.org/10.1177/0361198118784384.

Figueroa Medina, A. M., and A. P. Tarko. 2007. "Speed changes in the vicinity of horizontal curves on two-lane rural roads." *J. Transp. Eng.* 133 (4): 215–222. https://doi.org/10.1061/(ASCE)0733-947X(2007)133:4(215).

Fitzpatrick, K., et al. 2000. *Speed prediction for two-lane rural highways*. Rep. No. FHWA-RD-99-171. Washington, DC: Federal Highway Administration.

Fitzpatrick, K., and J. M. Collins. 2000. "Speed-profile model for two-lane rural highways." *Transp. Res. Rec.* 1737 (1): 42–49. https://doi.org/10.3141/1737-06.

Fitzsimmons, E. J., S. S. Nambisan, R. R. Souleyrette, and V. Kvam. 2013. "Analyses of vehicle trajectories and speed profiles along horizontal curves." *J. Transp. Saf. Secur.* 5 (3): 187–207. https://doi.org/10.1080/19439962.2012.680573.

Garber, N., and L. Hoel. 2015. *Traffic and highway engineering*. 5th ed. Stamford, CT: Cengage Learning.

Gareth, J., W. Daniela, H. Trevor, and T. Robert. 2013. *An introduction to statistical—Learning: With applications in R*. New York: Springer.

Hashim, I. H., T. A. Abdel-Wahed, and Y. Moustafa. 2016. "Toward an operating speed profile model for rural two-lane roads in Egypt." *J. Traffic Transp. Eng.* 3 (1): 82–88. https://doi.org/10.1016/j.jtte.2015.09.005.

Imran, M., Y. Hassan, and D. Patterson. 2006. "GPS–GIS-Based procedure for tracking vehicle path on horizontal alignments." *Comput.-Aided Civ. Infrastruct. Eng.* 21 (5): 383–394. https://doi.org/10.1111/j.1467-8667.2006.00444.x.

Jacob, A., and M. V. L. R. Anjaneyulu. 2013. "Operating speed of different classes of vehicles at horizontal curves on two-lane rural highways." *J. Transp. Eng.* 139 (3): 287–294. https://doi.org/10.1061/(ASCE)TE.1943-5436.0000503.

Jacob, B., and E. Violette. 2012. "Vehicle trajectory analysis: An advanced tool for road safety." *Procedia Social Behav. Sci.* 48 (2): 1805–1814. https://doi.org/10.1016/j.sbspro.2012.06.1155.

Kabacoff, R. I. 2011. *R in action: Data analysis and graphics with R*. 2nd ed. New York: Manning Publications.

Krammes, R. A., R. Q. Brackett, M. A. Shafer, J. L. Ottesen, I. B. Anderson, K. L. Fink, K. M. Collins, O. J. Pendleton, and C. J. Messer. 1995. *Horizontal alignment design consistency for rural two-zlane highways*. FHWA-RD-94-034. McLean, VA: Federal Highway Administration.

Lamm, R., E. M. Choueiri, and J. C. Hayward. 1988. "Tangent as an independent design element." *Transp. Res. Rec.* 1195 (1): 123–131.

Llopis-Castelló, D., F. Bella, F. J. Camacho-Torregrosa, and A. García. 2018a. "New consistency model based on inertial operating speed profiles for road safety evaluation." *J. Transp. Eng. Part A Syst.* 144 (4): 04018006. https://doi.org/10.1061/JTEPBS.0000126.

Llopis-Castelló, D., F. J. Camacho-Torregrosa, and A. García. 2018b. "Development of a global inertial consistency model to assess road safety on Spanish two-lane rural roads." *Accid. Anal. Prev.* 119 (4): 138–148. https://doi.org/10.1016/j.aap.2018.07.018.

Malaghan, V., D. S. Pawar, and H. Dia. 2020a. "Modeling operating speed using continuous speed profiles on two-lane rural highways in India." *J. Transp. Eng. Part A Syst.* 146 (11): 04020124. https://doi.org/10.1061/JTEPBS.0000447.

Malaghan, V., D. S. Pawar, and H. Dia. 2020b. "Speed prediction models for heavy passenger vehicles on rural highways based on an instrumented vehicle study." *Transp. Lett.* 2020 (1): 1–10. https://doi.org/10.1080/19427867.2020.1811005.

Malaghan, V., D. S. Pawar, and H. Dia. 2021a. "Exploring maximum and minimum operating speed positions on road geometric elements using continuous speed data." *J. Transp. Eng. Part A Syst.* 147 (8): 04021039. https://doi.org/10.1061/JTEPBS.0000539.

Malaghan, V., D. S. Pawar, and H. Dia. 2021b. "Modeling acceleration and deceleration rates for two-lane rural highways using global positioning system data." *J. Adv. Transp.* 2021 (1): 030876. https://doi.org/10.1155/2021/6630876.

McFadden, J., and L. Elefteriadou. 2000. "Evaluating horizontal alignment design consistency of two-lane rural highways: Development of new procedure." *Transp. Res. Rec.* 1737 (1): 9–17. https://doi.org/10.3141/1737-02.

Memon, R. A., G. B. Khaskheli, and A. S. Qureshi. 2008. "Operating speed models for two-lane rural roads in Pakistan." *Can. J. Civ. Eng.* 35 (5): 443–453. https://doi.org/10.1139/L07-126.

Montella, A., F. Galante, L. L. Imbriani, F. Mauriello, and M. Pernetti. 2014a. "Simulator evaluation of drivers' behaviour on horizontal curves of two-lane rural highways." *Adv. Transp. Stud. Int. J.* 34 (Nov): 91–104.

Montella, A., L. Pariota, F. Galante, L. L. Imbriani, and F. Mauriello. 2014b. "Prediction of drivers' speed behavior on rural motorways based on an instrumented vehicle study." *Transp. Res. Rec.* 2434 (1): 52–62. https://doi.org/10.3141/2434-07.

MORTH (Ministry of Road Transport and Highways). 2019. *Road accidents in India 2019*. New Delhi, India: MORTH.

Ottesen, J. L., and R. A. Krammes. 2000. "Speed-profile model for a design-consistency evaluation procedure in the United States." *Transp. Res. Rec.* 1701 (1): 76–85. https://doi.org/10.3141/1701-10.

Passetti, K. A., and D. B. Fambro. 1999. "Operating speeds on curves with and without spiral transitions." *Transp. Res. Rec.* 1658 (1): 9–16. https://doi.org/10.3141/1658-02.

Pérez Zuriaga, A. M., A. Garcia Garcia, F. J. Camacho-Torregrosa, and P. D'Attoma. 2010. "Modeling operating speed and deceleration on two-lane rural roads with global positioning system data." *Transp. Res. Rec.* 2171 (1): 11–20. https://doi.org/10.3141/2171-02.

Pérez-Zuriaga, A. M., F. J. Camacho-Torregrosa, and A. García. 2013. "Tangent-to-curve transition on two-lane rural roads based on continuous speed profiles." *J. Transp. Eng.* 139 (11): 1048–1057. https://doi.org/10.1061/(ASCE)TE.1943-5436.0000583.

Russo, F., S. A. Biancardo, and M. Busiello. 2016. "Operating speed as a key factor in studying the driver behaviour in a rural context." *Transport* 31 (2): 260–270. https://doi.org/10.3846/16484142.2016.1193054.

Sil, G., S. Nama, A. Maji, and A. K. Maurya. 2020. "Modeling 85th percentile speed using spatially evaluated free-flow vehicles for consistency based geometric design." *J. Transp. Eng. Part A Syst.* 146 (2): 04019060. https://doi.org/10.1061/JTEPBS.0000286.

Spacek, P. 2005. "Track behavior in curve areas: Attempt at typology." *J. Transp. Eng.* 131 (9): 669–676. https://doi.org/10.1061/(ASCE)0733-947X(2005)131:9(669).

Stodart, B. P., and E. T. Donnell. 2008. "Speed and lateral vehicle position models from controlled nighttime driving experiment." *J. Transp. Eng.* 134 (11): 439–449. https://doi.org/10.1061/(ASCE)0733-947X(2008)134:11(439).

TRB (Transportation Research Board) Operational Effects of Geometrics Committee. 2011. *Modeling operating speed: Synthesis report*. Washington, DC: Transportation Research Circular.

Wang, B., S. Hallmark, P. Savolainen, and J. Dong. 2018. "Examining vehicle operating speeds on rural two-lane curves using naturalistic driving data." *Accid. Anal. Prev.* 118 (4): 236–243. https://doi.org/10.1016/j.aap.2018.03.017.

Wang, J., K. K. Dixon, H. Li, and M. Hunter. 2006. "Operating-speed model for low-speed urban tangent streets based on in-vehicle global positioning system data." *Transp. Res. Rec.* 1961 (1): 24–33. https://doi.org/10.1177/0361198106196100104.

Wang, X., Q. Guo, and A. P. Tarko. 2020. "Modeling speed profiles on mountainous freeways using high resolution data." *Transp. Res. Part C Emerging Technol.* 117 (4): 102679. https://doi.org/10.1016/j.trc.2020.102679.

Zegeer, C. V., J. R. Steward, F. M. Council, D. W. Reinfurt, and E. Hamilton. 1992. "Safety effects of geometric improvements on horizontal curves." *Transp. Res. Rec.* 1356 (1): 11–19.